Supporting Information

Couto et al. 10.1073/pnas.1217428110

SI Materials and Methods

Strains Used. The wild-type reference strain was N2 Bristol; other strains are listed in order of appearance: AX2061, N2 *dbEx[pgcy-37::cGi500]*; AX204, *npr-1(ad609)*; AX2089, *npr-1(ad609) dbEx [pgcy-37::cGi500]*; AX2067, *gcy-35(ok769) dbEx[pgcy-37::cGi500]*; AX2237, *unc-13(e51) dbEx[pgcy-37::cGi500]*; AX2082, *pde-1(db40) dbEx[pgcy-37::cGi500]*; AX2062, *cng-1(db111) dbEx[pgcy-37:: cGi500]*; AX2272, *pde-1(ok2924); npr-1(ad609)*; AX2235 *pde-1 (ok2924) dbEx[pgcy-37::cGi500]*; AX2255, *pde-1(ok2924); npr-1 (ad609) dbEx[pgcy-32::YC3.60]*; AX4237 *dbEx[pgcy-32::pde-1]*; AX2283, *tax-2(ot25) dbEx[pgcy-37::cGi500]*; AX2064, *tax-4(p678) dbEx[pgcy-37::cGi500]*; AX2273, *pde-1(ok2924); cng-1(db111) dbEx [pgcy-37::cGi500]*; AX2239, *pde-2(tm3098)*; *npr-1(ad609) dbEx [pgcy-32::YC3.60];* AX2257, *pde-2(tm3098) dbEx[pgcy-37::cGi500];* AX2246, *pde-1(ok2924); pde-2(tm3098) dbEx[pgcy-37::cGi500];* AX2258, *egl-4(n478); npr-1(ad609) dbEx[pgcy-32::YC3.60]*; AX2065, *egl-4(n478) dbEx[pgcy-37::cGi500];* AX4238 *egl-4(n478) dbEx [pgcy-37::cGi500] dbEx[pgcy-36::egl-4];* AX2240, *pde-2(tm3098); egl-4(n478) dbEx[pgcy-37::cGi500];* AX2216, *egl-4(n478); cng-1 (db111) dbEx[pgcy-37::cGi500];* and AX2247, *pde-1(ok2924) egl-4(n478) dbEx[pgcy-37::cGi500].*

Genetics. *The pde-1(db40)* allele was isolated in a CB4856 (Hawaii) genetic background as a suppressor of aggregation behavior in a screen of 20,000 haploid ethyl methanesulfonate (EMS) mutagenized genomes. The *db40* mutation was mapped to the right arm of chromosome I, between *lev-11* and *unc-75*, using standard methods. To refine its map position, we selected 90 Lev-non-Unc recombinant progeny from *db40/lev-11 unc-75* animals and, from these, picked animals that were homozygous for the recombinant chromosome. These were phenotyped for aggregation behavior, and the recombination breakpoint was mapped using SNP markers that distinguish N2 and CB4856 chromosomes. Three informative recombinants narrowed the physical location of *db40* between SNPs uCE1-1423 and pkP1134; sequencing analysis of coding regions in the region revealed a mutation in *pde-1*. Noncomplementation tests with *pde-1(ok2924)* confirmed that *db40* was an allele of *pde-1*.

Molecular Biology. The cGi500 sensor (1) was PCR amplified using AF132 and AF133 oligos (AF132 GGGGACAAGTTTGTACAAAAAAGCAGGCTCAACGTGCTGGTTATTGTGC; AF133 GGGGACCACTTTGTACAAGAAAGCTGGGTCAGTGGTATTTGTGAGCCAGG) sub- cloned into pDONR221 using the Gateway BP reaction (Multisite Gateway; Invitrogen). The resulting clone was named pAF-ENTR-21-cGMPs.

The promoter fragment of *gcy-37* (1.1 kb) was amplified using PCR from N2 genomic DNA with the AF82 and AF83 primers (AF82 GGGGACAACTTTGTATAGAAAAGTTGGCTAATAAGTATGATAACGCTGG; AF83 GGGGACTGCTTTTTTGTACAAACTTGTTACGAAATGCTGTGGTCC). The resulting fragment was cloned into pDONRP4-P1R using the BP reaction (Multisite Gateway; Invitrogen) to generate pAF-ENTR-15-pgcy37.

pAF-EXPR-26 was created by recombining pAF-ENTR-15-pgcy37, pAF-ENTR-21-cGMPs, pENTR-unc54 3′ UTR, and pDESTR4-R3 to create an expression plasmid that expressed the cGMP sensor under the control of the *gcy-37* promoter. This plasmid was injected at 60 ng/μL together with 1 kb DNA Ladder (Invitrogen) at 40 ng/μL to create transgenic lines expressing the sensor.

The cDNA from *pde-1* (1,995 bp) was amplified from an RNA prep using RT-PCR with the oAC1 and oAC2 primers (oAC1 GGGGACAGCTTTCTTGTACAAAGTGGAAAACTATGAACCGAGCTCGTAAAACC; oAC2 GGGGACAACTTTGTATAATAAAGTTGtcaattcgttgtgacgccattttc). The resulting fragment was cloned into pDONRP221 using the BP reaction (Multisite Gateway; Invitrogen) to generate pAF-ENTR-A.

pAF-EXPR-A was created by recombining pAF-ENTR-pgcy32, pAF-ENTRA-pde-1cDNA, pENTR-unc54 3′ UTR, and pDESTR4-R3 to create an expression plasmid that expressed the *pde-1* coding sequence under the control of the *gcy-32* promoter. This plasmid was injected at 50 ng/μL together with ccRFP for transgene selection at 60 ng/μL.

Behavioral Assays. About 30 young adult animals were picked onto a 5-cm NGM plate that had been seeded with OP50 *Escherichia coli* 24 h before the experiment. After 1 h, a polydimethylsiloxane (PDMS) chamber was placed over the worms. The chamber was connected to the gas supply (BOC U.K. Ltd) via PE50 polyethylene tubing (Intramedic). Gas was delivered at 3 mL/min by a syringe pump (PHD 2000; Harvard Apparatus). Teflon valves (Automated Scientific) allowed rapid and precise gas switch. Behavioral footage was obtained using a Grasshopper 20S4M-C CCD camera (Point Gray Research), and individual animals were tracked using DIAS (Solltech). A custom-written script in Matlab (Mathworks) calculated the speed of individual animals, and Microsoft Excel was used to calculate average and SEM and construct graphs, as previously described (2). For all behavioral data, assays were carried out on at least three different days, and statistical significance was determined using the two-tailed Student *t* test.

cGMP and Calcium Imaging. Young adult worms were tethered using surgical glue (Nexaband; WPI Inc.) to a 2% agarose pad in M9 Buffer. A Y-chamber laid over the animals was connected to a syringe pump (PHD 2000; Harvard Apparatus) that delivered defined gas mixtures (B.O.C.) at 3 mL/min. The samples were imaged using an Axiovert inverted compound microscope (Zeiss) equipped with a 40× C-Apochromat lens and Metamorph acquisition software (Molecular Devices). A 2.0 neutral density filter reduced photobleaching. Images were captured with 100 ms exposure time at 2 (for calcium) or 3 (for cGMP) frames per s. A custom-written script in Matlab (Mathworks) was used to construct mean fluorescent ratio graphs, and Microsoft Excel was used to calculate mean amplitude and baseline fluorescence. Simultaneous imaging of cGMP and Ca^{2+} was carried out on a spinning disc confocal using a 40× objective lens (Nikon). Two EM-CCD cameras (Andor) coupled to the microscope using Andor's Tu-Cam first captured CFP and YFP fluorescence from cGi500, and then, 400 msec later, RFP fluorescence from R-GECO1. We used a 440-nm laser to excite cGi500, and a 561-nm laser to excite R-GECO1. We used a Di01-T445/515/561 excitation dichroic filter in the scan head. Since this dichroic lets in 3% of the 561-nm excitation light, we incorporated an FF01-485/537/627-25 filter in the light path, mounted in the Tu Cam cube to filter the light further. To collect the emission light, the Tu Cam TR-DCIS-CA1-00 Revolution cassette contained an FF509-FDi01 dichroic, and FF01-483/32 (CFP camera arm) and FF01-515/LP (YFP and R-GECO1 arm) filters. All filters were from Semrock. Images were captured at 1 fps. We used ImageJ to quantify acquired data.

Cell Culture. To monitor intracellular cAMP and cGMP levels by FRET, 293A cells (Invitrogen) were maintained under standard conditions and transfected using Effectene transfection reagent (Qiagen) with plasmids expressing Epac1-camps or cGi500 sensors and *Caenorhabditis elegans* PDE-1. Twenty-four hours after transfection, cells were washed once and maintained in a physiological buffer containing 144 mM NaCl, 5.4 mM KCl, 2 mM $CaCl_2$, 1 mM $MgCl_2$, and 20 mM Hepes, pH 7.4 at room temperature. Imaging was performed on a Zeiss Axio Observer A1 microscope equipped with Plan-Apochromat 63×/1.4 oil immersion objective, Polychrome V light source, DV2 Dual-View beam splitter, and CoolSNAP-HQ2 CCD-camera (Visitron Systems). Cells were stimulated with various ligands, and the YFP/CFP emission ratio following excitation with 436 nM light (emission filters were 535 ± 15 nm for YFP and 480 ± 20 nm for CFP) was monitored using VisiView software (Visitron). Emission values were corrected for bleedthrough of CFP into the YFP channel and for photobleaching. Imaging data were analyzed using Excel and Origin 8.5 (OriginLab) software packages.

1. Russwurm M, et al. (2007) Design of fluorescence resonance energy transfer (FRET)-based cGMP indicators: A systematic approach. *Biochem* 407(1):69–77.

2. Busch KE, et al. (2012) Tonic signaling from O_2 sensors sets neural circuit activity and behavioral state. *Nat Neurosci* 15(4):581–591.

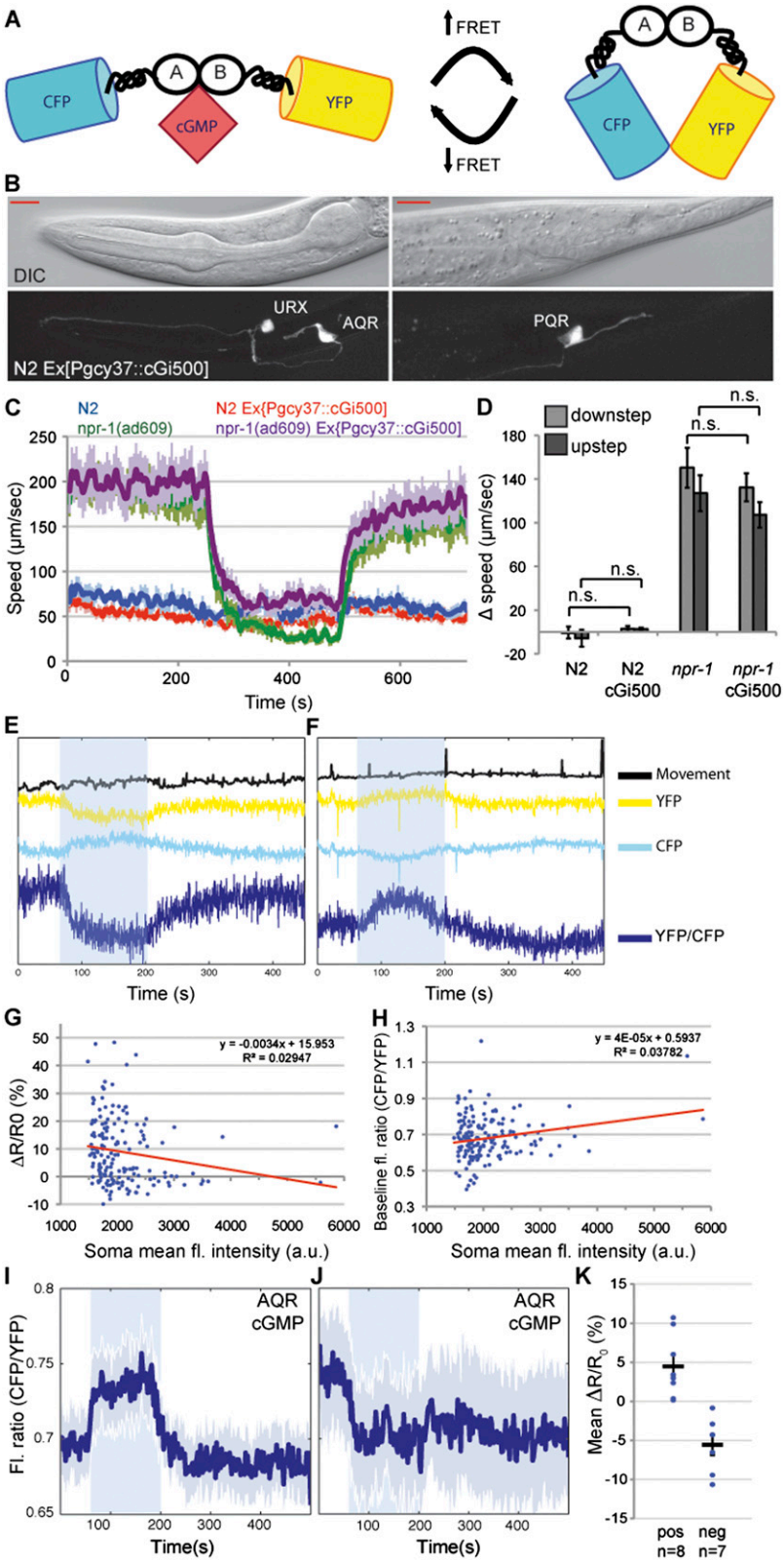

Fig. S1. The cGi500 cGMP sensor is distributed evenly in the O_2 sensing neurons PQR, AQR, and URX and does not compromise their function (related to Fig. 1). (*A*) Schematic diagram of the cGi500 cGMP sensor, consisting of CFP and YFP linked by the cGMP-binding domains (marked A and B) of cGMP-dependent protein kinase I (PKGI). Arrows indicate how changes in [cGMP] alter FRET between the fluorophores. (*B*) In vivo expression of cGi500 under the control of the *gcy-37* promoter. The reporter is expressed strongly and uniformly throughout the O_2 sensing neurons and does not elicit any obvious neuroanatomical abnormalities. (*Lower*) Two projections of confocal stacks of fluorescent images showing either the head neurons URX and AQR (*Left*) or a tail neuron PQR (*Right*). (*Upper*) A single DIC picture for orientation. The worm is oriented dorsal up and anterior left. (Scale bar: 10 µm.) (*C*) Animals expressing cGi500

Legend continued on following page

in O_2 sensors behave comparably to nontransformed animals when stimulated with different O_2 concentrations. N2 and N2 Ex[pgcy-37::cGi500] behave similarly and so do *npr-1(ad609)* and *npr-1(ad609)* Ex[Pgcy-37::cGi500]. The O_2 stimulus profile used was: 0–240 s, 21% O_2; 240–480 s, 7% O_2; 480–720 s, 21% O_2. Shading around traces indicate SEM. Number of assays was eight for all genotypes. (*D*) Quantification of data from *C* shows no significant differences between animals bearing the transgene and controls. For the downstep from 21% to 7% O_2, the difference in average speed is calculated as $S_f - S_o$, where S_f is the average speed during the last minute at 7% (420–480 s) and S_o the average speed during the last minute at 21% (180–240 s). For the O_2 upstep, S_f is the average speed during the last minute at 21% (660–720 s) and S_o the average speed during the last minute at 7% (420–480 s). Error bars indicate SEM. n.s., not significantly different (two-tailed Student *t* test). (*E* and *F*) O_2-evoked changes in fluorescence ratio YFP/CFP reflect reciprocal changes in the YFP and the CFP signals. This reciprocity is true both for positive (*E*) and negative (*F*) signals. Black traces indicate worm movement. Blue shadowing indicates 21% O_2, and no shadowing indicates 7% O_2. (*G* and *H*) Fluorescence intensity in the soma of PQR of animals expressing cGi500 does not correlate with the amplitude of FRET responses (*G*) or fluorescence ratio at baseline when animals where exposed to 7% O_2 (*H*). Blue dots represent individual recordings from PQR of wild-type worms expressing cGi500. Red line is a trend line. (*I–K*) O_2-evoked cGMP responses in AQR neuron. *I* shows an average trace of rising cGMP levels upon O_2 stimulation whereas *J* shows an average trace of decreasing cGMP levels under the same experimental conditions. *K* is a quantification of dR/R_0 from *I* and *J*.

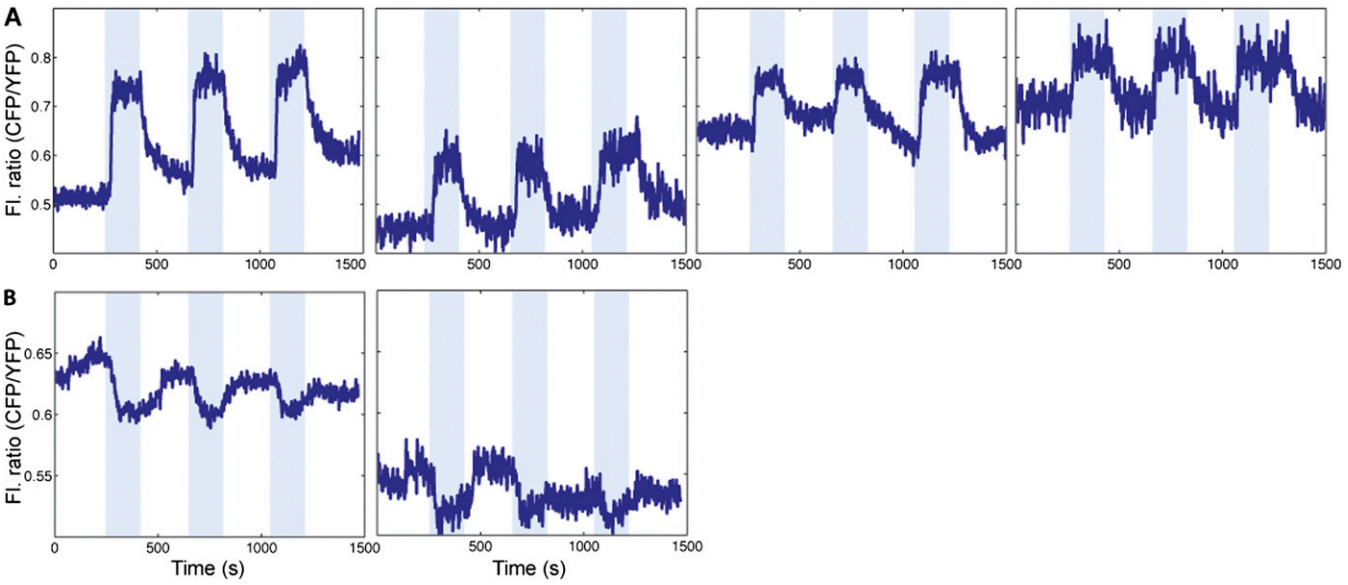

Fig. S2. Animal-to-animal variation reflects differences in neural state (related to Fig. 2). (*A* and *B*) Individual cGMP traces under a repeated stimulation protocol show that individual worms consistently exhibit either positive (*A*) or negative (*B*) cGMP responses, suggesting animal-to-animal differences in PQR neural state rather than intrinsic variability in cGMP signal transduction. Blue shadowing indicates 21% O_2, and no shadowing indicates 7% O_2.

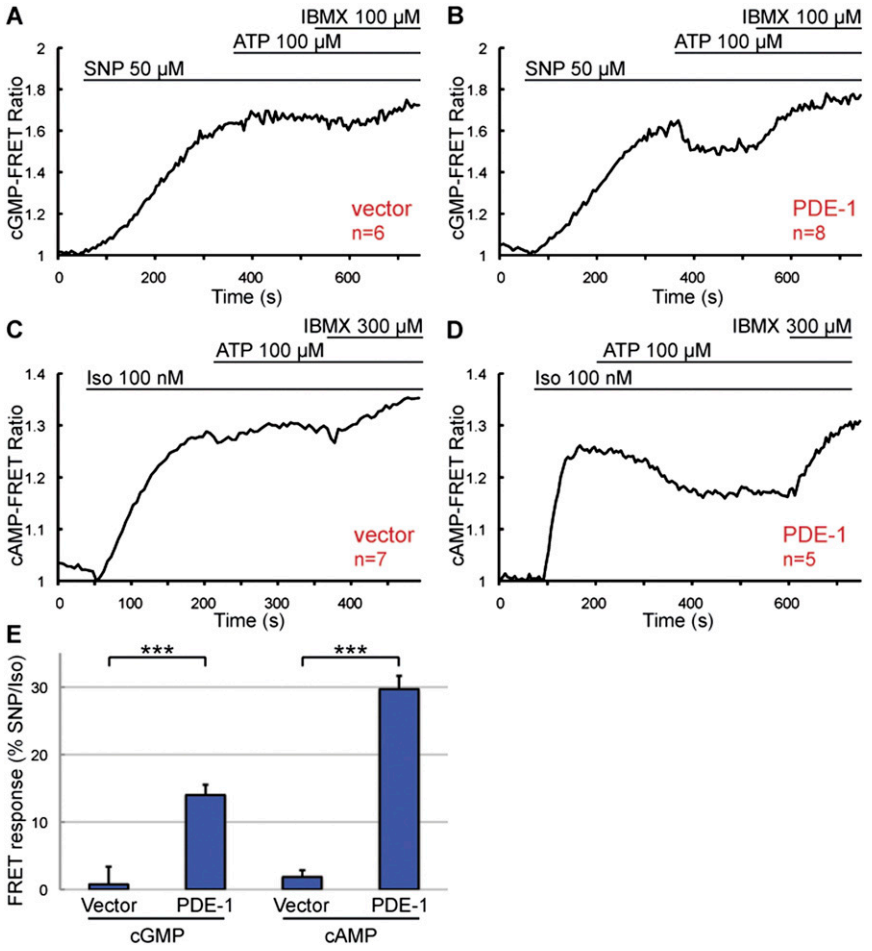

Fig. S3. PDE-1 is a Ca^{2+}-stimulated dual specificity phosphodiesterase. (*A* and *B*) Comparison of changes in [cGMP] evoked in HEK293A cells transfected with empty vector (*A*) and vector expressing PDE-1 (*B*). Sodium nitroprusside (SNP) stimulates production of cGMP, ATP stimulates Ca^{2+} entry, and IBMX inhibits phosphodiesterase activity. (*C* and *D*) Comparison of changes in [cAMP] evoked in HEK293A cells transfected with empty vector (*C*) and vector expressing PDE-1 (*D*). Isoproterenol (Iso) stimulates production of cAMP, ATP stimulates Ca^{2+} entry, and IBMX inhibits phosphodiesterase activity. (*E*) Quantification of results shown in *A*–*D*.

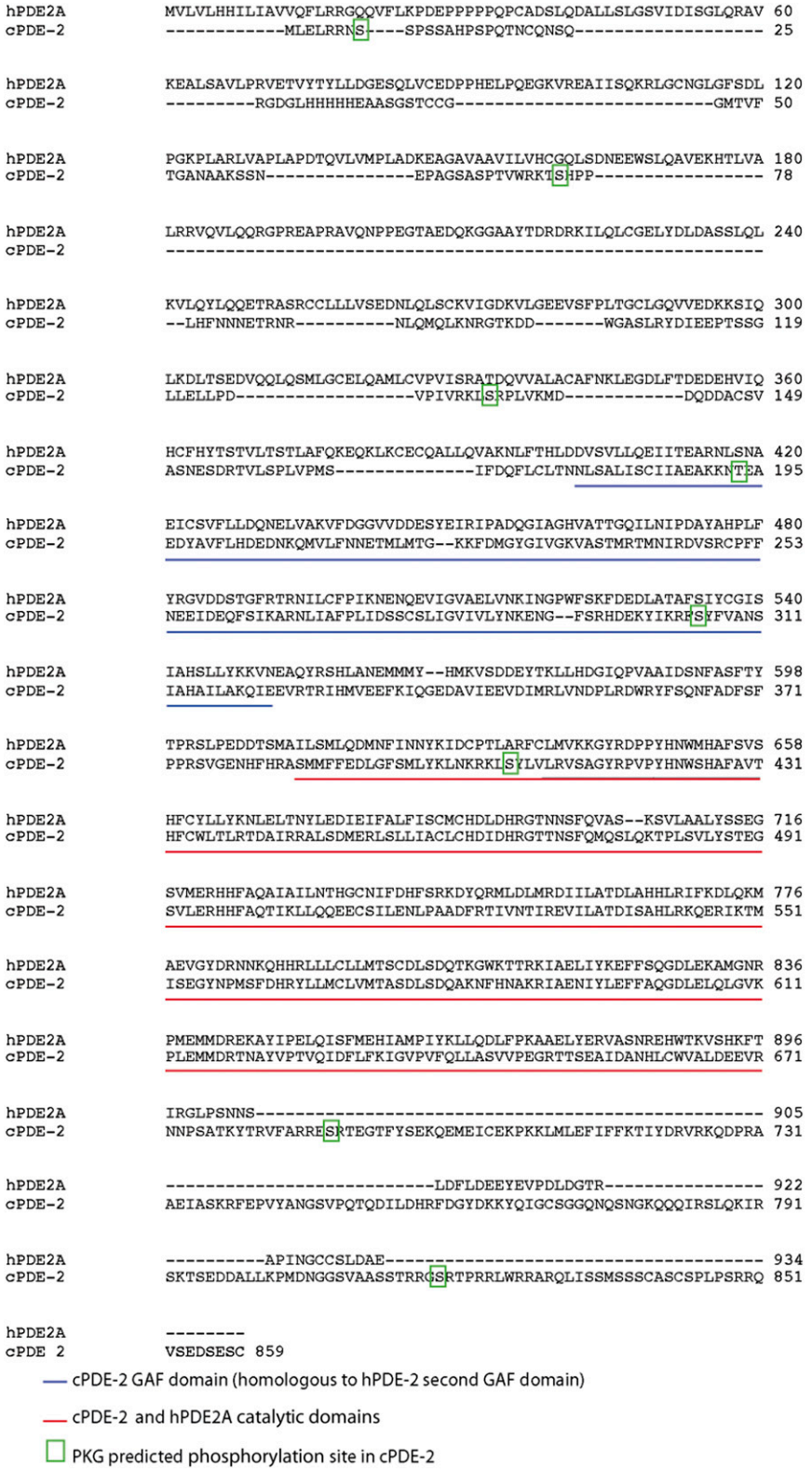

Fig. S4. *C. elegans* PDE-2, which is homologous to vertebrate PDE2A, contains a GAF domain and several predicted PKG phosphorylation sites. ClustalW alignment shows homology between *C. elegans* PDE-2 and human PDE2A sequences. Blue line underlines PDE-2 GAF domain and hPDE2A GAF B domain. Red line underlines the catalytic domain in both homologous sequences. Green squares indicate predicted PKG phosphorylation sites.